EPJ Web of Conferences **287**, 09003 (2023) https://doi.org/10.1051/epjconf/202328709003
EOSAM 2023

Linewidth-narrowing and frequency noise reduction of Brillouin fiber laser cavity operating at 1-µm

Moise Deroh[1,*], *Erwan* Lucas[2], *Kamal* Hammani[1], *Guy* Millot[1, 2], and *Bertrand* Kibler[1]

[1]Laboratoire Interdisciplinaire Carnot de Bourgogne, UMR 6303 CNRS, Université de Bourgogne (UB), Dijon, France
[2]Institut Universitaire de France (IUF), 1 Rue Descartes, Paris, France

Abstract. We report on a stabilized single-frequency Brillouin fiber laser operating at 1.06 µm by means of a passive highly nonlinear fiber ring cavity combined with a phase-locking loop scheme. We show significant linewidth narrowing (below 1-kHz) as well as frequency noise reduction compared to that of the initial pump in our mode-hop free Brillouin fiber laser.

Stimulated Brillouin Scattering (SBS) in optical waveguides is a nonlinear effect that occurs when the optical field interacts with acoustic waves through electrostriction and photoelastic phenomena [1]. The Brillouin process has been extensively leveraged for many important applications. Among these, we distinguish Brillouin lasers [2], which have attracted significant interest as ultra-high coherence light sources with sub-Hertz linewidth in simple all-fiber passive optical cavities [3] and in high-Q microresonators [4] suitable for applications in optical communications and LIDAR systems. To date, most of Brillouin lasers have been designed to operate in the telecom bands. However, there is a need to develop narrow-linewidth, low-noise and high-power laser sources at shorter wavelengths for applications covering this spectral region such as coherent communications and sensing.

In this contribution, we demonstrate a stabilized single-frequency and mode-hope free Brillouin fiber laser (BFL) operating around 1-µm based on a highly nonlinear germanosilicate fiber cavity.

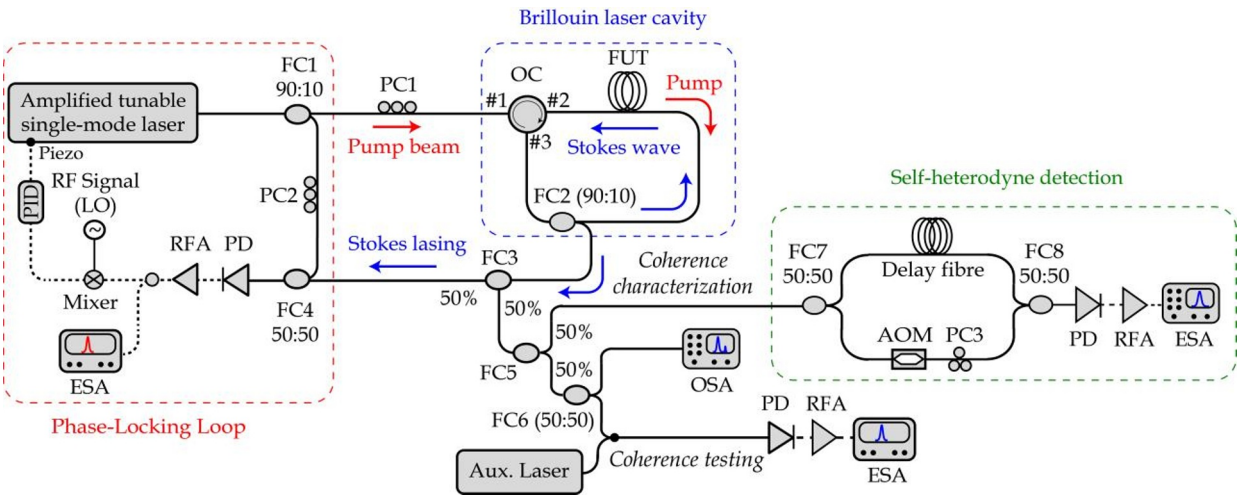

Fig. 1 Experimental setup of BFL cavity (blue dot) combined with a phase-locked stabilization loop diagram (red dot). Self-delayed heterodyne detection (green dot) used for coherence properties characterization. PC: Polarization controller, OC: Optical circulator, FC: Fiber coupler, FUT: Fiber under test, RFA: Radio-frequency amplifier, OSA: Optical spectrum analyzer, ESA: Electrical spectrum analyzer, PD: Photodiode, LO: Local oscillator, PID: Proportional-integral-derivative controller, AOM: Acousto-optic modulator.

Figure 1 depicts the complete experimental setup used for both implementation and characterization of our stabilized BFL with a standard non-resonant pumping configuration. An amplified narrow-linewidth continuous-wave laser tunable from 1.039 to 1.075 µm (Toptica DLC-PRO-025563) was used as a pump laser. This pump laser was then split into two parts. The first part is injected into the highly-nonlinear germanosilicate fiber (FUT: fiber under test) that forms the cavity using an optical circulator. A 90:10 fiber tap coupler was inserted to extract and characterize the BFL signal while the remaining 90% of the Stokes wave was fed back into the passive fiber ring cavity. The second part of the laser is used to create a beatnote with the Stokes laser. This beatnote is stabilized to an external oscillator via a phase-locking loop (PLL) that feeds back on the laser wavelength [5]. This suppresses the thermal drift of our fiber cavity relative to the pump laser.

First, we characterized stimulated Brillouin scattering at 1-µm pump wavelength in three distinct doped-core optical

* Corresponding author: koffi.deroh@u-bourgogne.fr

fibers with increasing GeO_2 content. Our results clearly reveal an enhancement of the Brillouin gain efficiency in heavily GeO_2 core-doped fibers compared to that of standard silica single-mode fibers. Concomitantly, the Brillouin frequency shift is tuned over more than 4 GHz with a strong decrease from 15.95 GHz (SMF-28) down to 11.87 GHz (ultra-high doping level, 75 mol.% GeO_2). The spectral width of the Brillouin gain also widens strongly up to 69.7 MHz, with the increase of the GeO_2 core content [6]. We then selected the most suitable fiber to form our 1-µm Brillouin fiber laser.

Next, we implemented the Brillouin fiber cavity with a 15-m long segment of HNLF-1 fiber. The fiber length was chosen as a trade-off between the gain-loss balance in the ring cavity and the number of cavity modes. The cavity finesse and free spectral range (FSR) were estimated to be 3.3 and 12.8 MHz respectively. In Fig. 2 (a), we show the Stokes power as a function of the input pump power for both SMF-28 (3.6 mol.% GeO_2) and HNLF-1 (21 mol.% GeO_2) fibers. Despite using a shorter fiber, the HNLF-1 BFL has a 140 mW threshold, which is lower than that of the SMF-28-based BFL. The inset of figure 2 (a) depicts the evolution of the BFL spectra (HNLF-1 fiber cavity) operating around 1 µm. Below the Stokes lasing operation, we clearly see the presence of reflected pump mainly coming from both Fresnel reflections and Rayleigh scattering. By increasing the injected power, the Stokes lasing occurs (blue spectra) as an upper wavelength shift of 50 pm, that matches the SBS frequency. Fig. 2 (b) exhibits the beating signal between the pump source and Brillouin laser recorded with 51 kHz of resolution bandwidth with an excellent coherent single-frequency lasing emission. We further investigated the coherence properties of our Brillouin laser. The phase and frequency noises of both BFL and pump laser were also characterized based on the self-heterodyne interferometer and a digital RF coherent receiver [7] as described in Fig. 2 (c). The measurement noise floor was characterized by measuring the frequency noise of the voltage-controlled oscillator driving the AOM (black curve). Across the measurement range, the Stokes laser frequency noise (blue curve) exhibits a stark reduction compared to that of the pump laser (red curve). For instance, at 100 kHz offset frequency, a noise reduction of 32 dB was observed. To estimate the integrated linewidth of the BFL and pump laser from the noise measurements, we used the common beta-separation line criterion. An integrated linewidth of ~ 10 kHz was obtained for the initial pump laser, while the Stokes laser frequency noise yields a narrower integrated linewidth of 1 kHz. The theoretical value of the Brillouin laser linewidth was expected to be about 200 Hz. The discrepancy between our measurement and theoretical prediction of BFL linewidth can be ascribed to the additional technical noise arising from cavity fluctuations. Finally, we used the low-noise features of our BFL laser as an optical frequency reference to characterize an auxiliary laser operating at 1.06 µm (see Fig. 2 (d)). Current efforts are deployed to reduce linear cavity losses and increase the lasing efficiency, as well as implement a dual-frequency pumping of the cavity to generate Kerr frequency comb through four-wave mixing processes, in similar way to Ref. [8].

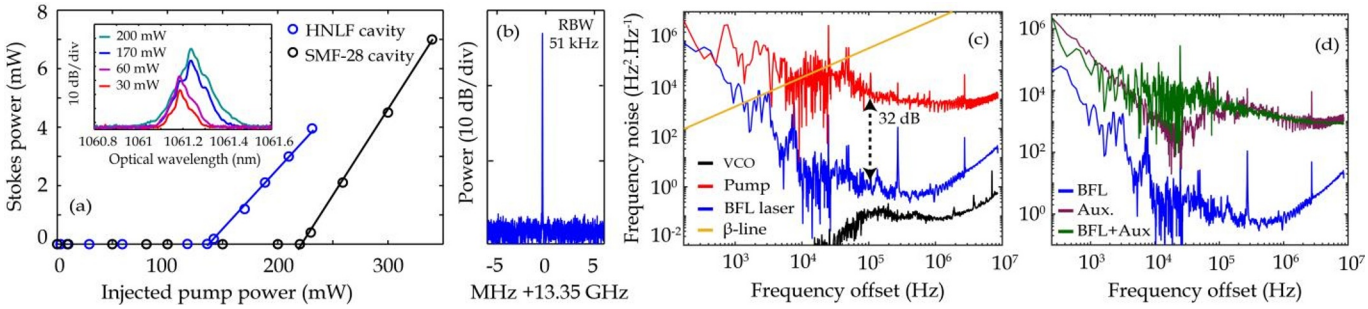

Fig 2. (a) First order Stokes lasing threshold measurement of both HNLF-1 21 mol.% (15-m long segment, blue circle) and SMF-28 fiber (44-m long segment, black circle). Inset: Experimental Brillouin laser optical spectra dynamics with the HNLF-1 21 mol.% fiber by varying injected pump power. (b) The beatnote of pump source and Brillouin laser, showing an excellent coherent single frequency emission. (c) Frequency noise measurement of the voltage-controlled reference oscillator (VCO) of AOM, pump source, Brillouin laser and auxiliary laser source. The β-separation (solid line, in yellow) shows the intersection with the frequency noise curves, useful for estimating the integrated linewidth. (d) Comparison of Brillouin laser frequency noise with auxiliary laser and beat-note noise

References

1. G. P. Agrawal, (Academic Press, 2019).
2. K. O. Hill, B. S. Kawasaki, and D. C. Johnson, Appl. Phys. Lett. **28**, 608 (1976).
3. S. Gundavarapu, G. M. Brodnik, M. Puckett, T. Huffman, D. Bose, R. Behunin, J. Wu, T. Qiu, C. Pinho, N. Chauhan, J. Nohava, P. T. Rakich, K. D. Nelson, M. Salit, and D. J. Blumenthal, Nat. Photonics **13**, 60 (2019).
4. W. Loh, S. Yegnanarayanan, F. O'Donnell, and P. W. Juodawlkis, Optica **6**, 152 (2019).
5. G. Danion, L. Frein, D. Bacquet, G. Pillet, S. Molin, L. Morvan, G. Ducournau, M. Vallet, P. Szriftgiser, and M. Alouini, Opt. Lett. **41**, 2362 (2016).
6. M. Deroh, B. Kibler, H. Maillotte, T. Sylvestre, and J.-C. Beugnot, Opt. Lett. **43**, 4005 (2018).
7. L. Richter, H. Mandelberg, M. Kruger, and P. McGrath, IEEE J. Quantum Electron. **22**, 2070 (1986).
8. E. Lucas, M. Deroh, and B. Kibler, arXiv (2022).